


Temperature-dependent layer breathing modes in two-dimensional materials

Indrajit Maity, Prabal K. Maiti, and Manish Jain*

Department of Physics, Indian Institute of Science, Bangalore-560012, India

 (Received 5 January 2018; revised manuscript received 29 March 2018; published 24 April 2018)

Relative out-of-plane displacements of the constituent layers of two-dimensional materials give rise to unique low-frequency breathing modes. By computing the height-height correlation functions from molecular dynamics simulations, we show that the layer breathing modes (LBMs) can be mapped consistently to vibrations of a simple linear chain model. Our calculated thickness dependence of LBM frequencies for few-layer (FL) graphene and molybdenum disulfide (MoS_2) are in excellent agreement with available experiments. Our results show a redshift of LBM frequency with an increase in temperature, which is a direct consequence of anharmonicities present in the interlayer interaction. We also predict the thickness and temperature dependence of LBM frequencies for FL hexagonal boron nitride. Our Rapid Communication provides a simple and efficient way to probe the interlayer interaction for layered materials and their heterostructures with the inclusion of anharmonic effects.

DOI: [10.1103/PhysRevB.97.161406](https://doi.org/10.1103/PhysRevB.97.161406)

Two-dimensional (2D) materials, for example, graphene, transition-metal dichalcogenides, and hexagonal boron nitride (hBN), are being studied extensively for their exciting electronic, thermal, and mechanical properties [1,2]. A great deal of effort has also been directed towards understanding hybrid structures of these 2D materials [3]. It is well known that typically a few layers of 2D materials and their hybrid structures are coupled by weak van der Waals (VDW) forces. Such layer-layer couplings give rise to unique low-frequency *interlayer* vibrational modes at finite temperatures, namely, shear and layer breathing modes (LBMs). [4,5]. It has been found experimentally that LBMs are more sensitive to external perturbations than shear modes [6]. These LBMs can be used as a direct probe to determine layer thickness, stacking order, effects of external environment, adsorbates, etc. [6–18]. Furthermore, LBMs play a crucial role in interlayer electric conductance [19] and thermoelectric transport [20]. Understanding the origin and quantification of LBM frequencies is thus of immense practical importance.

Three key features emerge from the low-frequency Raman spectroscopic measurements of LBMs in 2D materials: (i) A system with n layers will have $n - 1$ *distinct* LBMs [21]. (ii) LBM frequencies (at the Γ point) are highly sensitive to the thickness of the material, i.e., the number of layers. For instance, when the number of layers of graphene is increased from 2 to 8, the lowest LBM frequency redshifts from 81 to 22 cm^{-1} [6]. (iii) The lowest LBM frequency also redshifts with an increment of temperature (T) as seen in experiments by controlled laser heating [6,13]. The reported linewidths in Raman spectroscopic measurements for LBMs are typically larger than shear modes [11]. These observations suggest the presence of strong anharmonicity in the interlayer interaction for LBMs. In this Rapid Communication, we address these three key aspects of LBMs.

A 2D material embedded in three-dimensional space can have out-of-plane acoustic phonon mode called flexural mode (ZA). In the harmonic approximation, this flexural mode has a dispersion $\omega_{\text{flex}} \propto q^2$ for small momentum q . For n layers, due to interlayer coupling, the degeneracy in the ZA branch is lifted, and *distinct* modes appear in the vibrational spectra, implying vertical stretching/compression of the layers. These modes are known as LBMs (ZO' , optical modes). In order to understand the thickness dependence of LBMs, two common approaches are used. First, a linear chain model of n masses with a nearest-neighbor interaction is used widely to determine LBM frequencies. This simple model has been shown to predict the frequencies accurately, given a knowledge of nearest-neighbor layer coupling [6,7,10,11]. However, the mapping of the n -layer system to such a simple model starting from a more general description of the constituent layers is unclear. The effects of next-nearest-neighbor layer coupling in such a model have not been quantified as well. Second, first-principles calculations based on density functional perturbation theory (DFPT) are frequently used to calculate LBM frequencies [10,22]. In these calculations, however, the temperature dependence of LBMs is not revealed. The inclusion of anharmonic effects, i.e., multiphonon processes and thermal expansion coefficients are necessary to capture the temperature dependence of LBM frequencies.

Here, we present a simple method to calculate LBM frequencies by using a combination of classical molecular dynamics (MD) simulations and the theory of membranes. We justify the application of the linear chain model in the small momentum regime ($q \rightarrow 0$) by computing the height-height correlations from MD simulations. Our calculations of the layer dependence of the LBM frequencies for few-layer graphene and MoS_2 are in excellent agreement with available experiments. We show the evolution of the LBM frequency with temperature for the bilayer (BL) system of graphene, MoS_2 , and hBN. In the studied temperature (T) range, we find expansion of interlayer separation and redshift in LBM frequency with a T increment. As the interlayer

*mjain@iisc.ac.in

separation is calculated directly from the MD simulation, *all* anharmonicities in the interlayer interaction are incorporated in the calculation.

We perform MD simulations with the periodic boundary condition in the *NPT* (where N is number of atoms per layer and P is the pressure) ensemble using a Nosé-Hoover thermostat and barostat as implemented in LAMMPS [23]. We simulate three different layered materials, namely, graphene, MoS₂, and hBN and vary the number of layers from 2 to 6. Initially, all the samples are chosen to be roughly square shaped and contain ≈ 8000 – 9000 atoms per layer (N). After equilibration, we use 4000 snapshots (a 2-ns production run) to average the calculated properties. We use different force fields (FFs) to compute the LBM frequencies. For graphene three different FFs are adopted: the long-range bond order potential for carbon (LCBOP) [24], a combination of the reactive empirical bond order potential and the Lennard-Jones potential (REBO + LJ) [25,26], and DREIDING, a more generic FF [27]. For the case of MoS₂ and hBN, a mix of the Stillinger-Weber and Lennard-Jones potential (SW + LJ) [28–30] and DREIDING are used, respectively.

The applicability of the theory of membranes (a continuum description) to understand long-wavelength physics in 2D materials, such as graphene, is now well established [31–33]. In the harmonic approximation of membrane theory, the bending energy for a BL system with weak VDW interaction between the layers can be written as

$$E_{BL} = \frac{1}{2} \int [\kappa(\nabla^2 h_1)^2 + \kappa(\nabla^2 h_2)^2 + \sigma(h_1 - h_2)^2] d^2x, \quad (1)$$

where κ is the bending rigidity of each constituent layer, h_1, h_2 are the heights of two layers with respect to each of their reference plane, and σ denotes the interlayer coupling. In the momentum space, using the combinations of $h = (h_1 + h_2)/\sqrt{2}$ and $\delta h = (h_1 - h_2)/\sqrt{2}$, one can identify two modes: the *mean* and the *fluctuation* modes. The corresponding height correlation functions [34] are

$$H^{BL}(q) = \langle |h(q)|^2 \rangle = \frac{Nk_B T}{S_0 \kappa q^4}, \quad (2)$$

$$\delta H^{BL}(q) = \langle |\delta h(q)|^2 \rangle = \frac{Nk_B T}{S_0(\kappa q^4 + 2\sigma)}, \quad (3)$$

where S_0 is the surface area per atom and $q = |\vec{q}|$ is defined by the dimension of the simulation box. The dispersion relations for the long-wavelength physics can be inferred from the above relations: $\omega_{\text{mean}} = \sqrt{\frac{\kappa}{\rho}} q^2$ and $\omega_{\text{fluc}} = \sqrt{\frac{\kappa q^4 + 2\sigma}{\rho}}$, where ρ is the two-dimensional mass density [see the Supplemental Material (SM) [35]]. It should be noted that quantum effects are neglected in the calculation of height correlation functions [$H^{BL}(q)$, $\delta H^{BL}(q)$]. Although the effects are important at low T , these effects are reported to be unimportant above a crossover temperature of $T^* \sim 70$ – 90 K [33]. All the correlation functions presented here are calculated for $T \geq 150$ K from MD simulations, hence, quantum effects can be neglected.

Figure 1(a) shows height correlation functions per atom [$H^{BL}(q)/N$, $\delta H^{BL}(q)/N$] for the *mean* and the *fluctuation*

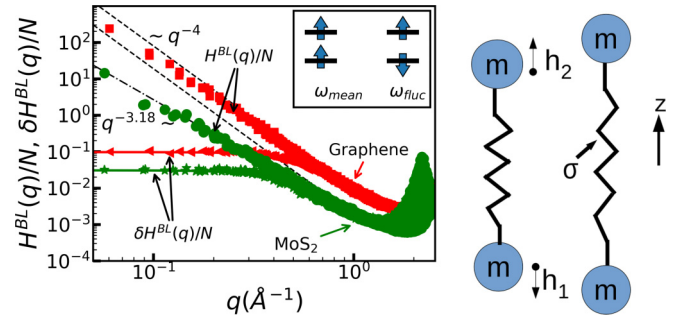


FIG. 1. (a) Height correlation functions for the *mean* mode $H^{BL}(q)/N$ (graphene: the red squares; MoS₂: the green circles) and the *fluctuation* mode $\delta H^{BL}(q)/N$ (graphene: the red triangles; MoS₂: the green stars) for BL graphene and BL MoS₂ using MD simulations. The black dashed and dashed-dotted lines show scaling q^{-4} , $q^{-3.18}$ respectively. The solid lines denote the fit to the *fluctuation* mode. The inset shows schematics of normal modes at the Γ point. (b) The linear chain model: two masses (m) connected by a spring with spring constant σ .

modes in BL graphene and MoS₂ at room temperature. In the figure we have shown the results for BL graphene using the REBO + LJ and for BL MoS₂ using the SW + LJ. However, the main features of the height correlation functions are insensitive to the choice of force fields. The *mean* mode of BL graphene is well described within the harmonic approximation [Eq. (2)] for $0.5 \text{ \AA}^{-1} \leq q \leq 1.0 \text{ \AA}^{-1}$. The membrane theory predicts a change in scaling from $H^{BL}(q) \propto q^{-4}$ to $H^{BL}(q) \propto q^{-3.18}$ when anharmonicities become important owing to the coupling of bending and stretching [36]. This deviation from the harmonic approximations of membrane theory, i.e., a change in scaling from $H^{BL}(q) \sim q^{-4}$, is found in all the simulated samples. Our results show that anharmonic effects are more pronounced in BL MoS₂ compared to that of graphene [Fig. 1(a)]. More generally, we find the *mean* mode of the BL system behaves like a single layer for all the simulated materials. The *fluctuation* mode for both BL graphene and MoS₂ becomes a constant for $q \lesssim 0.2 \text{ \AA}^{-1}$. This implies that near the zone center (Γ point) the interlayer coupling (σ) dictates the height fluctuations as predicted by Eq. (3). This aspect of the *fluctuation* mode is key for the rest of our Rapid Communication. Contrary to the *mean* mode, for small q , the anharmonicities arising from the coupling between bending and stretching are found to be irrelevant for the *fluctuation* mode. The *fluctuation* mode is identified with the LBM. For $q > 1.0 \text{ \AA}^{-1}$, we find deviations from the membrane theory and the existence of Bragg peaks. These peaks [Fig. 1(a)] signify the underneath crystal lattice structure. This is reasonable as we are using MD simulated data of crystals and fitting them with the continuum theory of membranes.

For $q \rightarrow 0$, $\omega_{\text{mean}} \rightarrow 0$, and $\omega_{\text{fluc}} \rightarrow \sqrt{\frac{2\sigma}{\rho}}$, we identify ω_{fluc} as the LBM frequency (ZO') of a BL system. This *dispersionless* feature of ω_{fluc} helps us in two significant ways: (i) We can estimate σ directly from the flat region of $\delta H^{BL}(q)$ without depending on any other mechanical parameter. (ii) The mapping of the BL system to the linear chain model [Fig. 1(b)] becomes transparent. In such a model, the force constants are determined solely from the interlayer coupling. The schematics

TABLE I. Comparison of force constants calculated from the MD simulation and the first-principles approach.

BL system	Temperature (K)	σ ($\times 10^{19}$ N m $^{-3}$)	Method
Graphene	300	8.1	REBO + LJ
		7.3	LCBOP
Graphene	0	7.9	DFPT [22]
MoS ₂	300	8.3	SW + LJ
MoS ₂	0	9.26	DFPT [10]

of the modes of the constituent layers at the Γ point are shown in the inset of Fig. 1(a). The interlayer interaction lifts the degeneracy of the flexural modes of each layer into ω_{mean} and ω_{fluc} for $q \rightarrow 0$. This can be confirmed from the differences of $\delta H^{BL}(q)/N$ and $H^{BL}(q)/N$. In Table I, we show the force constants for BL graphene and MoS₂ and compare those with the values obtained from first-principles calculations. As can be easily examined from the table, our results are in excellent agreement with earlier reports.

The generalization of the LBMs from a BL to a FL system can be performed in a similar fashion as in Eq. (1). Keeping only the nearest-neighbor layer coupling terms in the FL system, we find the normalized eigenvectors and use them to compute all the height correlation functions *explicitly* (see the SM [35]). We find the *mean* mode of the FL system behaves like a single layer for the studied sample sizes. Similar to the case of the BL system, the *fluctuation* modes are identified with the LBMs. In Fig. 2 we show the layer dependence of the LBM frequencies for graphene, MoS₂, and hBN. For a n -layer system, there are $(n - 1)$ distinct LBM frequencies. As can be seen from the figures, our results for graphene [Fig. 2(a)] and MoS₂ [Fig. 2(b)] capture the layer dependence accurately. The figures also show the LBM frequencies using DFPT [10,22]. Experimental data for graphene are shown only for the lowest LBM frequency as they dominate the Raman response [6]. The LBM with the lowest frequency displays an extraordinarily simple structure where constituent layers expand and compress with respect to the midlayer (odd n) or midpoint (even n). Qualitatively, this mode results in the least restoring force, hence, the lowest frequency (for the schematics see the SM [35]). With DREIDING, the frequencies

are overestimated by $\sim 28\%$ [Fig. 2(c)] for FL graphene. Although overestimated, the general trend for the thickness dependence of the LBM frequencies is similar for hBN and graphene, consistent with another prediction [37]. We cannot compare the LBM frequencies for hBN with the experimental data as the LBMs have not been characterized for hBN yet.

Two simple traits of the evolution of frequencies with thicknesses of 2D samples must be pointed out: (i) Upon increasing the number of layers, interlayer coupling between nearest-neighbor layers remains almost constant (within the error bar), consistent with an earlier report [22]. Thus, by computing σ from the BL system and using a simple linear chain model the dramatic redshifts of the lowest frequency of the LBMs with thicknesses can be captured *without calculating explicitly* the height fluctuation modes for the FL sample. (ii) The effect of the next-nearest-neighbor interaction is found to be negligible for all the simulated samples (see the SM [35]). If the coupling is significant enough, this method can be easily applied by adding more terms to the bending energy and reevaluating the height fluctuation correlations with normalized eigenvectors.

So far, in the bending energy cost [Eq. (1)] for a BL system, both the interlayer and the intralayer interaction terms are assumed to be harmonic. As is well known, at constant P , upon heating the material, the volume changes. This change in volume can be explained via inclusion of anharmonic terms in the Hamiltonian. Also the change in phonon frequency (ω) with T can only be obtained from the anharmonicities of the potential energy. We calculate the change in the LBM frequency with T , $\chi = \frac{d\omega}{dT}$, the first-order temperature coefficient, to discern the anharmonic effects in the interlayer interaction. In this regard, we also compute the thermal expansion coefficient for interlayer separation $\alpha_{\perp} = \frac{1}{c} \frac{dc}{dT}$. All the reported values are estimated for the BL system with T well below the melting point.

Figure 3 shows the temperature dependence of interlayer separation and the LBM frequency for BL graphene with REBO + LJ and the DREIDING FF. Our results show that the equilibrium spacing between layers c increases with T ($\alpha_{\perp} > 0$). Moreover, increasing T leads to the softening of the *effective spring constant* σ of the harmonic oscillator. This results in a redshift ($\chi < 0$) of the LBM frequency, which can also be substantiated from Table II. All the anharmonic effects are automatically included in our calculation of σ . In principle,

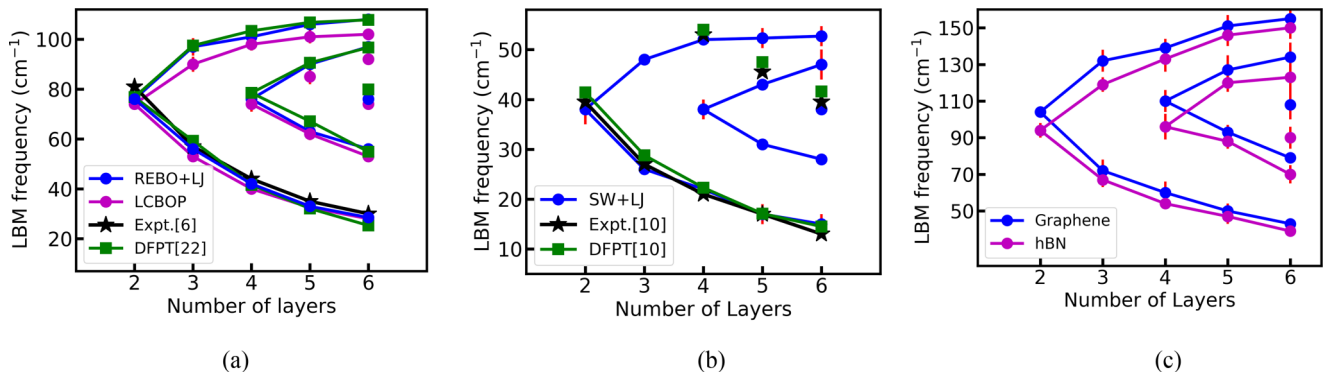


FIG. 2. Thickness dependence of LBM frequencies. (a) FL graphene, (b) FL MoS₂, and (c) comparison of FL graphene and FL hBN calculated using the DREIDING [27] force field. The solid lines are used as a guide to the eye. The vertical lines (red) denote error bars.

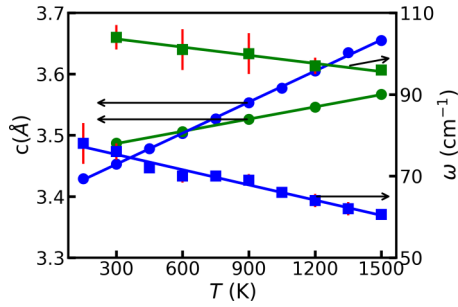


FIG. 3. Change in interlayer spacing c (left scale) and LBM frequency ω (right scale) with T . The blue (green) circles present variation of c using the REBO + LJ (DREIDING), and the blue squares (green squares) show the evolution of ω using the REBO + LJ (DREIDING). The solid lines represent linear fits to the data.

χ can be grouped into two parts: a “self-energy” shift due to direct anharmonic coupling of the phonon modes χ_V and a shift because of the volume change in the material χ_T [13,38]. As all our simulations are carried out at constant P , both contributions are included in the estimated χ . The second-order temperature coefficient is found to be irrelevant in the studied temperature range. In Table II, we have shown α_{\perp} for BL systems and compared it to the bulk values [39]. With standard DREIDING parameters α_{\perp} is always underestimated compared to more accurate FFs. We find that α_{\perp} for the BL (with accurate FFs) is larger than that of the bulk (experiments). It is interesting to note that there is a difference in the order of magnitude for α_{\perp} ($\sim 10^{-5} \text{ K}^{-1}$) and the in-plane expansion coefficient α_{\parallel} ($\sim 10^{-6} \text{ K}^{-1}$). This is consistent with earlier observations [40,41]. However, the fact that α_{\perp} is greater than α_{\parallel} is not very surprising. This is due to the difference in strengths of interlayer and intralayer interactions of 2D materials.

To summarize, we have analyzed out-of-plane vibrations of 2D materials using a combination of classical molecular dynamics simulations and membrane theory. We report our

TABLE II. The effect of anharmonicity is to increase the interlayer spacing and redshift of the LBM frequency. The thermal expansion coefficients are shown at $T = 300 \text{ K}$.

Material	Method	α_{\perp} ($\times 10^{-5} \text{ K}^{-1}$)	χ ($\times 10^{-3} \text{ cm}^{-1} \text{ K}^{-1}$)
BL	REBO + LJ	4.9 ± 0.2	-12.4 ± 0.8
Graphene	DREIDING	1.9 ± 0.1	-6 ± 1
	LCBOP	6.2 ± 0.3	-22.6 ± 0.9
Graphite	Expt. [42]	2.7	
BL MoS ₂	SW + LJ	2.4 ± 0.3	-9.4 ± 1.4
Bulk MoS ₂	DFPT [43]	1.1	
BL hBN	DREIDING	2.3 ± 0.1	-6.7 ± 0.8
Bulk hBN	Expt. [41]	3.77	

results for three different classes of 2D materials, namely, graphene, MoS₂, and hBN. We provide a consistent way to map the LBMs of a few layers of stacked 2D materials to a simple linear chain model in the long-wavelength limit. The thickness sensitivity of the LBM frequencies at the Γ point are well captured and in agreement with earlier reports. We also find a redshift of the LBM frequency upon increasing T . We compute the interlayer separation thermal expansion coefficient along with the shift in LBM frequency for the BL systems. We show that with accurate FFs LBM frequencies can be reliably estimated within this simple picture. Our method also provides a framework to capture pressure or any other external environmental effects on the LBM frequencies. This Rapid Communication opens up the possibility for efficiently computing LBM frequencies (including anharmonic effects) to characterize and understand properties of 2D materials and their heterostructures.

The authors thank the Supercomputer Education and Research Center (SERC) at IISc for providing computational resources. The authors also thank G. K. Gupta for comments on the Rapid Communication.

- [1] K. S. Novoselov, V. Fal, L. Colombo, P. Gellert, M. Schwab, K. Kim *et al.*, *Nature (London)* **490**, 192 (2012).
- [2] S. Z. Butler, S. M. Hollen, L. Cao, Y. Cui, J. A. Gupta, H. R. Gutiérrez, T. F. Heinz, S. S. Hong, J. Huang, A. F. Ismach *et al.*, *ACS Nano* **7**, 2898 (2013).
- [3] A. K. Geim and I. V. Grigorieva, *Nature (London)* **499**, 419 (2013).
- [4] P. Tan, W. Han, W. Zhao, Z. Wu, K. Chang, H. Wang, Y. Wang, N. Bonini, N. Marzari, N. Pugno *et al.*, *Nature Mater.* **11**, 294 (2012).
- [5] L. Liang, J. Zhang, B. G. Sumpter, Q.-H. Tan, P.-H. Tan, and V. Meunier, *ACS Nano* **11**, 11777 (2017).
- [6] C. H. Lui, Z. Ye, C. Keiser, X. Xiao, and R. He, *Nano Lett.* **14**, 4615 (2014).
- [7] C. H. Lui and T. F. Heinz, *Phys. Rev. B* **87**, 121404 (2013).
- [8] R. He, T.-F. Chung, C. Delaney, C. Keiser, L. A. Jauregui, P. M. Shand, C. Chancey, Y. Wang, J. Bao, and Y. P. Chen, *Nano Lett.* **13**, 3594 (2013).
- [9] X. Zhang, W. P. Han, J. B. Wu, S. Milana, Y. Lu, Q. Q. Li, A. C. Ferrari, and P. H. Tan, *Phys. Rev. B* **87**, 115413 (2013).
- [10] Y. Zhao, X. Luo, H. Li, J. Zhang, P. T. Araujo, C. K. Gan, J. Wu, H. Zhang, S. Y. Quek, M. S. Dresselhaus *et al.*, *Nano Lett.* **13**, 1007 (2013).
- [11] M. Boukhicha, M. Calandra, M.-A. Measson, O. Lancry, and A. Shukla, *Phys. Rev. B* **87**, 195316 (2013).
- [12] J. Yan, J. Xia, X. Wang, L. Liu, J.-L. Kuo, B. K. Tay, S. Chen, W. Zhou, Z. Liu, and Z. X. Shen, *Nano Lett.* **15**, 8155 (2015).
- [13] X. Ling, L. Liang, S. Huang, A. A. Puretzy, D. B. Geohegan, B. G. Sumpter, J. Kong, V. Meunier, and M. S. Dresselhaus, *Nano Lett.* **15**, 4080 (2015).
- [14] Y. Zhao, X. Luo, J. Zhang, J. Wu, X. Bai, M. Wang, J. Jia, H. Peng, Z. Liu, S. Y. Quek *et al.*, *Phys. Rev. B* **90**, 245428 (2014).
- [15] H. Li, J.-B. Wu, F. Ran, M.-L. Lin, X.-L. Liu, Y. Zhao, X. Lu, Q. Xiong, J. Zhang, W. Huang, H. Zhang, and P.-H. Tan, *ACS Nano* **11**, 11714 (2017).

- [16] R. He, J. van Baren, J.-A. Yan, X. Xi, Z. Ye, G. Ye, I.-H. Lu, S. Leong, and C. Lui, *2D Mater.* **3**, 031008 (2016).
- [17] R. He, J.-A. Yan, Z. Yin, Z. Ye, G. Ye, J. Cheng, J. Li, and C. Lui, *Nano Lett.* **16**, 1404 (2016).
- [18] C. H. Lui, Z. Ye, C. Ji, K.-C. Chiu, C.-T. Chou, T. I. Andersen, C. Means-Shively, H. Anderson, J.-M. Wu, T. Kidd *et al.*, *Phys. Rev. B* **91**, 165403 (2015).
- [19] V. Perebeinos, J. Tersoff, and P. Avouris, *Phys. Rev. Lett.* **109**, 236604 (2012).
- [20] P. S. Mahapatra, K. Sarkar, H. R. Krishnamurthy, S. Mukerjee, and A. Ghosh, *Nano Lett.* **17**, 6822 (2017).
- [21] There is no periodicity in the out-of-plane (z) direction of the FL system. The Γ - A branch of the bulk counterpart is nonexistent in the Brillouin zone. One can show the frequencies of the LBMs at the Γ point for the FL system are associated with vibrations of their bulk correspondent along the Γ - A direction.
- [22] S. K. Saha, U. V. Waghmare, H. R. Krishnamurthy, and A. K. Sood, *Phys. Rev. B* **78**, 165421 (2008).
- [23] S. Plimpton, *J. Comput. Phys.* **117**, 1 (1995).
- [24] J. H. Los and A. Fasolino, *Phys. Rev. B* **68**, 024107 (2003).
- [25] D. W. Brenner, O. A. Shenderova, J. A. Harrison, S. J. Stuart, B. Ni, and S. B. Sinnott, *J. Phys.: Condens. Matter* **14**, 783 (2002).
- [26] L. A. Girifalco, M. Hodak, and R. S. Lee, *Phys. Rev. B* **62**, 13104 (2000).
- [27] S. L. Mayo, B. D. Olafson, and W. A. Goddard, *J. Phys. Chem.* **94**, 8897 (1990).
- [28] J.-W. Jiang, H. S. Park, and T. Rabczuk, *J. Appl. Phys.* **114**, 064307 (2013).
- [29] T. Liang, S. R. Phillpot, and S. B. Sinnott, *Phys. Rev. B* **79**, 245110 (2009).
- [30] T. Liang, S. R. Phillpot, and S. B. Sinnott, *Phys. Rev. B* **85**, 199903(E) (2012).
- [31] D. Nelson, T. Piran, and S. Weinberg, *Statistical Mechanics of Membranes and Surfaces* (World Scientific, Singapore, 2004).
- [32] A. Fasolino, J. Los, and M. I. Katsnelson, *Nature Mater.* **6**, 858 (2007).
- [33] B. Amorim, R. Roldán, E. Cappelluti, A. Fasolino, F. Guinea, and M. I. Katsnelson, *Phys. Rev. B* **89**, 224307 (2014).
- [34] This is the height-height correlation in momentum space. For convenience, we write it as the height correlation function.
- [35] See Supplemental Material at <http://link.aps.org/supplemental/10.1103/PhysRevB.97.161406> for the derivations of equations of motion corresponding to height fluctuations, height correlations for the single layer system (Sec. A), the bilayer system (Sec. B), the trilayer system (Sec. C), and the generalization to the n -layer system (Sec. D).
- [36] P. Le Doussal and L. Radzihovsky, *Phys. Rev. Lett.* **69**, 1209 (1992).
- [37] K. H. Michel and B. Verberck, *Phys. Rev. B* **85**, 094303 (2012).
- [38] C. Postmus, J. R. Ferraro, and S. S. Mitra, *Phys. Rev.* **174**, 983 (1968).
- [39] The value of α_{\perp} and χ for MoS₂ is calculated by changing T from 150 to 450 K only.
- [40] N. Mounet and N. Marzari, *Phys. Rev. B* **71**, 205214 (2005).
- [41] W. Paszkowicz, J. Pelka, M. Knapp, T. Szyszko, and S. Podsiadlo, *Appl. Phys. A* **75**, 431 (2002).
- [42] A. Bailey and B. Yates, *J. Appl. Phys.* **41**, 5088 (1970).
- [43] C. K. Gan and Y. Y. F. Liu, *Phys. Rev. B* **94**, 134303 (2016).